BEM & NFSI Conference Proceedings
Minneapolis, MN • May 12-15, 2005

Influence of High-Rank Background Interference on Adaptive Beamformer Source Reconstruction

K. Sekihara[1], K. Hild[2], S. S. Nagarajan[2]
[1]Department of Systems Engineering, Tokyo Metropolitan University, Tokyo, Japan
[2]Department of Radiology, University of California, San Francisco, CA, USA

Abstract – **This paper discusses the influence of the background brain activity on the adaptive beamformer reconstruction. By modeling the background activity as uniformly distributed incoherent sources, we derive the resolution kernel (point-spread function) of the minimum-variance adaptive beamformer and we show that the spatial resolution of the source reconstruction can be severely degraded by such background activities. We then propose two novel adaptive beamformer techniques that can reduce the influence from such background activities: the prewhitened eigenspace beamformer and covariance difference beamformer. We present numerical examples that show the effectiveness of these methods.**

Keywords – **Adaptive beamformer, Background activity, MEG, Random dipole model, Source reconstruction**

I. Introduction

One major problem with the EEG/MEG measurements is that measured MEG signal generally contains interference magnetic fields generated from background spontaneous activities, which are often referred to as the brain noise or the physiological noise. Such spontaneous activities generally degrade the quality of the source reconstruction results, and often make interpretating the reconstruction results difficult. This is particularly true for adaptive beamformer source reconstruction methods [1,2] because the high-rank nature of the background spontaneous activity [3,4] may invalidate the underlying low-rank signal assumption necessary for formulating the adaptive beamformers. This paper discusses the influence of such high-rank background brain activity on the results of the source reconstruction obtained using adaptive beamformer methods. We show that the spatial resolution can be severely degraded as an influence of such high-rank background activities. We then propose two novel adaptive beamformer methods that can restore the spatial resolution degraded by the background activities.

II. Definition and spatial filter formation

We define the magnetic field measured by the mth detector coil at time t as $b_m(t)$, and a column vector $\boldsymbol{b}(t) = [b_1(t), b_2(t), \ldots, b_M(t)]^T$ as a set of measured data where M is the total number of sensor coils and superscript T indicates the matrix transpose. The spatial location is represented by a three-dimensional vector $\boldsymbol{r}$: $\boldsymbol{r} = (x, y, z)$. The covariance matrix of the measurement is denoted $\boldsymbol{R}$, i.e., $\boldsymbol{R} = \langle \boldsymbol{b}(t)\boldsymbol{b}^T(t) \rangle$. The magnitude of the source moment is denoted $s(\boldsymbol{r}, t)$. We define the sensor lead field matrix, which represents the sensitivity of the whole sensor array at $\boldsymbol{r}$, as $\boldsymbol{L}(\boldsymbol{r}) = [\boldsymbol{l}_x(\boldsymbol{r}), \boldsymbol{l}_y(\boldsymbol{r}), \boldsymbol{l}_z(\boldsymbol{r})]$, where $\boldsymbol{l}_\zeta(\boldsymbol{r})$ (where ζ equals x, y, or z) is defined as $\boldsymbol{l}_\zeta(\boldsymbol{r}) = [l_1^\zeta(\boldsymbol{r}), l_2^\zeta(\boldsymbol{r}), \cdots, l_M^\zeta(\boldsymbol{r})]^T$, and $l_m^\zeta(\boldsymbol{r})$ is the output of the mth sensor induced by the unit-magnitude source located at $\boldsymbol{r}$ and pointing in the ζ direction.

The beamformer techniques estimate the source current density by computing $\widehat{s}(\boldsymbol{r}, t) = \boldsymbol{w}^T(\boldsymbol{r})\boldsymbol{b}(t)$ where $\widehat{s}(\boldsymbol{r}, t)$ is the estimated source magnitude. The column vector $\boldsymbol{w}(\boldsymbol{r})$ expresses a set of the filter weights. The weight vector of the minimum-variance beamformer, which is the best-known adaptive beamformer, is expressed as

$$\boldsymbol{w}(\boldsymbol{r}) = \frac{\boldsymbol{R}^{-1}\boldsymbol{l}(\boldsymbol{r})}{\boldsymbol{l}^T(\boldsymbol{r})\boldsymbol{R}^{-1}\boldsymbol{l}(\boldsymbol{r})}, \tag{1}$$

where $\boldsymbol{l}(\boldsymbol{r})$ is defined as $\boldsymbol{l}(\boldsymbol{r}) = \boldsymbol{L}(\boldsymbol{r})\boldsymbol{\eta}_{opt}(\boldsymbol{r})$. Here, $\boldsymbol{\eta}_{opt}(\boldsymbol{r})$ is the optimum direction determined as the direction that gives the maximum filter outputs.

III. Resolution kernel under background interference

We assume that the background sources are quasi-continuously distributed, and its magnitude and its orientation are denoted $\xi(\boldsymbol{r}, t)$ and $\boldsymbol{\eta}(\boldsymbol{r})$, respectively. Let us also assume that a single target source exists at $\boldsymbol{r}_1$ with an orientation equal to $\boldsymbol{\eta}_1$. Its magnitude is denoted $s(\boldsymbol{r}_1, t)$. Then, defining $\boldsymbol{f}$ such that $\boldsymbol{f} = \boldsymbol{L}(\boldsymbol{r}_1)\boldsymbol{\eta}_1$, the measured data $\boldsymbol{b}(t)$ is expressed as

$$\boldsymbol{b}(t) = s(\boldsymbol{r}_1, t)\boldsymbol{f} + \int \xi(\boldsymbol{r}, t)\boldsymbol{l}(\boldsymbol{r})d\boldsymbol{r} + \boldsymbol{n}(t), \tag{2}$$

where the lead field vector $\boldsymbol{l}(\boldsymbol{r})$ is defined such that $\boldsymbol{l}(\boldsymbol{r}) = \boldsymbol{L}(\boldsymbol{r})\boldsymbol{\eta}(\boldsymbol{r})$, and $\boldsymbol{n}(t)$ represents the sensor noise that are uncorrelated between different sensor channels.

The covariance matrix of the measurements is given by

$$\boldsymbol{R} = \sigma_1^2 \boldsymbol{f}\boldsymbol{f}^T + \int\int \langle \xi(\boldsymbol{r},t)\xi(\boldsymbol{r}',t)\rangle \boldsymbol{l}(\boldsymbol{r})\boldsymbol{l}(\boldsymbol{r}')d\boldsymbol{r}d\boldsymbol{r}' + \sigma_0^2\boldsymbol{I}, \tag{3}$$

where we define the signal power σ_1^2 such that $\sigma_1^2 = \langle s(\boldsymbol{r}_1,t)^2\rangle$, and use the relationship, $\langle \boldsymbol{n}(t)\boldsymbol{n}^T(t)\rangle = \sigma_0^2\boldsymbol{I}$. We assume that the background source activity is spatially uniform and incoherent, i.e.,

$$\langle \xi(\boldsymbol{r},t)\xi(\boldsymbol{r}',t)\rangle = \sigma_c^2\delta(\boldsymbol{r}-\boldsymbol{r}'), \tag{4}$$

where σ_c^2 is the power of the background source activity. Substituting the above equation into Eq. (3), we finally obtain

$$\boldsymbol{R} = \sigma_1^2\boldsymbol{f}\boldsymbol{f}^T + \sigma_c^2\boldsymbol{G} + +\sigma_0^2\boldsymbol{I}, \tag{5}$$

where $\boldsymbol{G}$ is the gram matrix defined as

$$\boldsymbol{G} = \int \boldsymbol{l}(\boldsymbol{r})\boldsymbol{l}^T(\boldsymbol{r})d\boldsymbol{r}. \tag{6}$$

The resolution kernel of the minimum-variance beamformer is expressed as,

$$\mathbb{R}(\boldsymbol{r},\boldsymbol{r}_0) = \boldsymbol{w}(\boldsymbol{r})\boldsymbol{f} = \frac{\boldsymbol{l}^T(\boldsymbol{r})\boldsymbol{R}^{-1}\boldsymbol{f}}{\boldsymbol{l}^T(\boldsymbol{r})\boldsymbol{R}^{-1}\boldsymbol{l}(\boldsymbol{r})}. \tag{7}$$

Substituting Eq. (5) into Eq. (7), we derive the resolution kernel normalized by its peak value such that

$$\mathbb{R}(\boldsymbol{r},\boldsymbol{r}_0) = \frac{\cos(\boldsymbol{l},\boldsymbol{f}|\boldsymbol{Q}^{-1})}{[1+\widetilde{\alpha}(1-\cos^2(\boldsymbol{l},\boldsymbol{f}|\boldsymbol{Q}^{-1}))]}, \tag{8}$$

where $\boldsymbol{Q} = \boldsymbol{I} + (\sigma_c^2/\sigma_0^2)\boldsymbol{G}$, $\widetilde{\alpha} = (\sigma_1^2/\sigma_0^2)\boldsymbol{f}\boldsymbol{Q}^{-1}\boldsymbol{f}^T$, and the generalized cosine is defined as $\cos^2(\boldsymbol{l},\boldsymbol{f}|\boldsymbol{Q}^{-1}) = (\boldsymbol{l}^T\boldsymbol{Q}^{-1}\boldsymbol{f})^2/[(\boldsymbol{l}^T\boldsymbol{Q}^{-1}\boldsymbol{l})(\boldsymbol{f}^T\boldsymbol{Q}^{-1}\boldsymbol{f})]$. In Section IV, we present numerical examples of the normalized resolution kernel obtained using the above equation, and show that, when increasing the power of the background activity, σ_c^2, a significant degradation of the spatial resolution is caused.

III. Separation of target activity from the background interference

We have developed two-types of novel beamformer techniques to extract the target activities from the background interference. To derive these techniques, we first assume that the control measurements which only contain the background interference are available, and the interference-plus-noise covariance matrix $\boldsymbol{R}_{i+n}$ can be obtained. Second, we assume that the background activities are stationary and they are uncorrelated with the target activities. Under this second assumption, we can derive the relationship

$$\boldsymbol{R} = \boldsymbol{R}_s + \boldsymbol{R}_{i+n}, \tag{9}$$

where $\boldsymbol{R}_s$ is the covariance matrix obtained from the signal magnetic field generated from the target sources only.

A. Prewhitened eigenspace beamformer

We define the prewhitened measurement covariance matrix $\widetilde{\boldsymbol{R}}$ as $\widetilde{\boldsymbol{R}} = \boldsymbol{R}_{i+n}^{-1/2}\boldsymbol{R}\boldsymbol{R}_{i+n}^{-1/2}$. Using Eq. (9), we have the relationship,

$$\widetilde{\boldsymbol{R}} = \boldsymbol{R}_{i+n}^{-1/2}\boldsymbol{R}_s\boldsymbol{R}_{i+n}^{-1/2} + \boldsymbol{I}. \tag{10}$$

We then define the eigenvalues and eigenvectors of $\widetilde{\boldsymbol{R}}$, respectively, as $\widetilde{\lambda}_1,\ldots,\widetilde{\lambda}_M$ and $\widetilde{\boldsymbol{e}}_1,\ldots,\widetilde{\boldsymbol{e}}_M$, and assume that P target sources exist. Then, according to Eq. (10), the P largest eigenvalues $\widetilde{\lambda}_1,\ldots,\widetilde{\lambda}_P$ are greater than 1 and related to the signal part $\boldsymbol{R}_{i+n}^{-1/2}\boldsymbol{R}_s\boldsymbol{R}_{i+n}^{-1/2}$, and other eigenvalues $\widetilde{\lambda}_{P+1},\ldots,\widetilde{\lambda}_M$ are equal to 1 and they are related to the interference and noise. Thus, we have,

$$\boldsymbol{R}_{i+n}^{-1/2}\boldsymbol{R}_s\boldsymbol{R}_{i+n}^{-1/2} = \sum_{j=1}^{P}\widetilde{\lambda}_j\widetilde{\boldsymbol{e}}_j. \tag{11}$$

Using the eigenvectors corresponding to these signal-level eigenvalues as $\widetilde{\boldsymbol{e}}_1,\ldots,\widetilde{\boldsymbol{e}}_P$, we define a matrix $\widetilde{\boldsymbol{E}}_S$ as $\widetilde{\boldsymbol{E}}_S = [\widetilde{\boldsymbol{e}}_1,\ldots,\widetilde{\boldsymbol{e}}_P]$. Then, using $\widetilde{\boldsymbol{E}}_S$, we define $\boldsymbol{\Pi}_S$ such that

$$\boldsymbol{\Pi}_S = \boldsymbol{R}_{i+n}^{1/2}\widetilde{\boldsymbol{E}}_S\widetilde{\boldsymbol{E}}_S^T\boldsymbol{R}_{i+n}^{-1/2}. \tag{12}$$

The weight vector of the prewhitened minimum-variance beamformer is obtained using $\boldsymbol{\Pi}_S$ as

$$\boldsymbol{w}_{pw}(\boldsymbol{r}) = \frac{\boldsymbol{\Pi}_S^T[\boldsymbol{\Pi}_S\boldsymbol{R}\boldsymbol{\Pi}_S^T + \gamma\boldsymbol{I}]^{-1}\boldsymbol{l}(\boldsymbol{r})}{\boldsymbol{l}^T(\boldsymbol{r})[\boldsymbol{\Pi}_S\boldsymbol{R}\boldsymbol{\Pi}_S^T + \gamma\boldsymbol{I}]^{-1}\boldsymbol{l}(\boldsymbol{r})}. \tag{13}$$

Note that $\boldsymbol{\Pi}_S\boldsymbol{R}\boldsymbol{\Pi}_S^T$ is expressed as

$$\begin{aligned}\boldsymbol{\Pi}_S\boldsymbol{R}\boldsymbol{\Pi}_S &= \boldsymbol{R}_{i+n}^{1/2}\widetilde{\boldsymbol{E}}_S\widetilde{\boldsymbol{E}}_S^T\boldsymbol{R}_{i+n}^{-1/2}\boldsymbol{R}[\boldsymbol{R}_{i+n}^{-1/2}\widetilde{\boldsymbol{E}}_S\widetilde{\boldsymbol{E}}_S^T\boldsymbol{R}_{i+n}^{1/2}]^T \\ &= \boldsymbol{R}_{i+n}^{1/2}[\widetilde{\boldsymbol{E}}_S\widetilde{\boldsymbol{E}}_S^T\widetilde{\boldsymbol{R}}]\boldsymbol{R}_{i+n}^{1/2}.\end{aligned}$$

According to Eq. (11), we have

$$[\widetilde{\boldsymbol{E}}_S\widetilde{\boldsymbol{E}}_S^T\widetilde{\boldsymbol{R}}] = \sum_{j=1}^{P}\widetilde{\lambda}_j\widetilde{\boldsymbol{e}}_j = \boldsymbol{R}_{i+n}^{-1/2}\boldsymbol{R}_s\boldsymbol{R}_{i+n}^{-1/2}, \tag{14}$$

and therefore the relationship

$$\boldsymbol{\Pi}_S\boldsymbol{R}\boldsymbol{\Pi}_S^T = \boldsymbol{R}_s \tag{15}$$

holds. That is, $\boldsymbol{\Pi}_S \boldsymbol{R} \boldsymbol{\Pi}_S^T + \gamma \boldsymbol{I}$ is approximately equal to the signal-plus-sensor-noise covariance matrix, and the prewhitening weight, $\boldsymbol{w}_{pw}^T(\boldsymbol{r})$, in Eq. (13) can provide an interference-free reconstruction of the target source activities.

B. Covariance difference beamformer

We next describe the other technique that directly uses the relationship in Eq. (9). Because we calculate the covariance matrices $\boldsymbol{R}$ and $\boldsymbol{R}_{i+n}$ from time samples, we cannot generally obtain the signal covariance matrix $\boldsymbol{R}_s$ by simply subtracting $\boldsymbol{R}_{i+n}$ from $\boldsymbol{R}$. This is because the numerically-obtained difference matrix $\Delta\boldsymbol{R}$: $\Delta\boldsymbol{R} = \boldsymbol{R} - \boldsymbol{R}_{i+n}$ and $\Delta\boldsymbol{R}^{-1}$ are not positive definite matrices and the quadratic form of $\Delta\boldsymbol{R}^{-1}$ can be negative. To derive the proposed beamformer's weight, we define the eigenvalues of $\Delta\boldsymbol{R}$ as $\gamma_1, \gamma_2, \ldots, \gamma_M$, and apply the eigenvalue decomposition to the difference matrix $\Delta\boldsymbol{R}$ such that

$$\Delta\boldsymbol{R} = \boldsymbol{U} \boldsymbol{\Upsilon} \boldsymbol{U}^T, \tag{16}$$

where $\boldsymbol{\Upsilon} = \mathrm{diag}[\gamma_1, \gamma_2, \ldots, \gamma_M]$ and diag[·] indicates a diagonal matrix. Here, $\boldsymbol{U}$ is an orthogonal matrix whose columns are the corresponding eigenvectors. We then define a matrix $\bar{\boldsymbol{\Upsilon}}$ such that $\bar{\boldsymbol{\Upsilon}} = \mathrm{diag}[|\gamma_1|, |\gamma_2|, \ldots, |\gamma_M|]$. The proposed covariance difference beamformer uses the positive definite matrix $\boldsymbol{U} \bar{\boldsymbol{\Upsilon}}^{-1} \boldsymbol{U}^T$, instead of using $\Delta\boldsymbol{R}^{-1}$, for deriving the weight. That is, the weight for the covariance difference beamformer is obtained as

$$\boldsymbol{w}_{diff}(\boldsymbol{r}) = \frac{\boldsymbol{E}_S \boldsymbol{E}_S^T \boldsymbol{R}^{-1} \boldsymbol{l}(\boldsymbol{r})}{\boldsymbol{l}^T(\boldsymbol{r}) [\boldsymbol{U} \bar{\boldsymbol{\Upsilon}}^{-1} \boldsymbol{U}^T] \boldsymbol{l}(\boldsymbol{r})}, \tag{17}$$

where $\boldsymbol{E}_S$ is a matrix whose columns are the eigenvectors corresponding to the signal-level eigenvalues of $\boldsymbol{R}$.

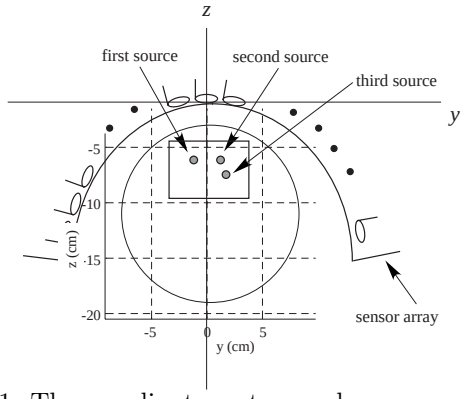

Figure 1: The coordinate system and source-sensor configuration used in the numerical experiments.

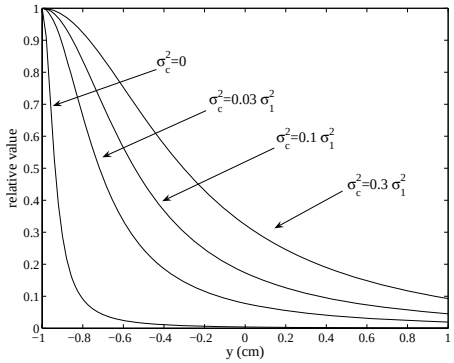

Figure 2: Plot of resolution kernels obtained using Eq. (8). Note that the maxima of these kernels are located at $y = -1$ because we assume that a single source exists at $(0, -1, -6)$.

IV. Numerical experiments

A sensor alignment of the 148-sensor array from Magnes 2500$^{\mathrm{TM}}$ (4D Neuroimaging Inc., San Diego) neuromagnetometer is used in our experiments. Three signal sources were assumed to exist on a single plane ($x =$ 0 cm). The source-sensor configuration and the coordinate system are illustrated in Fig. 1. First, we calculated the peak-normalized resolution kernel by using Eq. (8). Here, a single source was assumed to exist at $(0, -1, -6)$, the first source location, and the variance of the sensor noise, σ_0^2, is set at $\sigma_0^2 = (1/16)\sigma_1^2 \|\boldsymbol{f}\|^2/M$. Four different values of σ_c^2, $\sigma_c^2 = 0$, $\sigma_c^2 = 0.03\sigma_1^2$, $\sigma_c^2 = 0.1\sigma_1^2$, and $\sigma_c^2 = 0.3\sigma_1^2$ were used. The results are shown in Fig. 2 in which the kernel shape was plotted in the y direction. The results clearly show that when the power of the background interference σ_c^2 is increased, the spatial resolution is severely degraded.

The simulated magnetic recordings were calculated from -1200 to 1200 time points by assigning three time courses shown in Fig. 3(a) to the three sources. Here, we consider the data portion between -1200 and 0 is the prestimulus period and that between 0 and 1200 is the post-stimulus portion. Note that the third source is active for both the pre- and post-stimulus periods. A set of simulated magnetic recordings is shown in the upper panel of Fig. 3(b). We then generated another set of simulated magnetic recordings that contain the uniformly distributed incoherent activities. One hundred brain-noise sources with random locations and orientations were distributed, and magnetic fields from these sources were calculated by assuming that they had uncorrelated random time courses. These noise-source-originated magnetic fields are added to the recordings in the upper panel of Fig. 3(b). The final simulated mag-

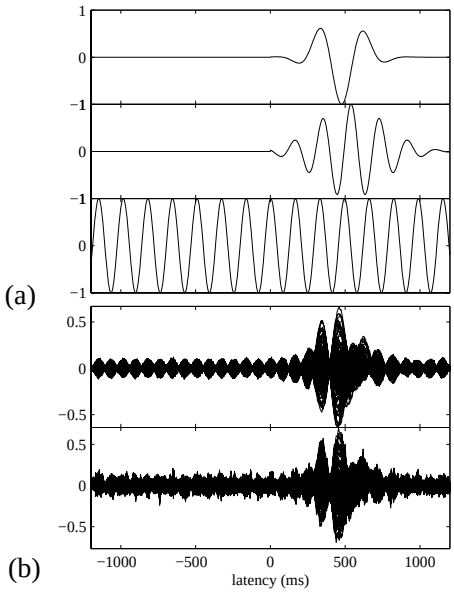

Figure 3: (a) Waveforms of the three sources assumed for the numerical experiments. (b) Generated magnetic recordings when no noise sources exist (upper) and when 100 noise sources exist (lower).

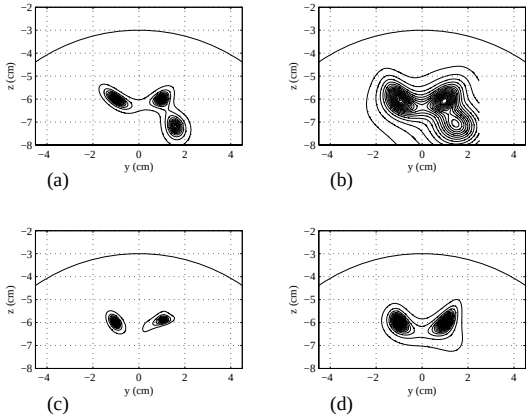

Figure 4: Conventional reconstruction (a) when no background source exists and (b) when background sources exist. (c) Prewhitened beamformer reconstruction, and (d) covariance difference beamformer reconstruction.

netic recordings are shown in the lower panel of Fig. 3(b). Note that we used the prestimulus period as the control period, the third source is considered as a control source in addition to the 100 noise sources. The first and the second sources are considered as the target sources.

The conventional minimum-variance beamformer in Eq. (1) was applied to these two sets of the simulated recordings. Here $\boldsymbol{R}$ was obtained using the whole poststimulus period. Figure 4(a) shows the results for the case with no background sources, and figure 4(b) shows the results for the case with 100 noise sources. The comparison between them also confirms that the background high-rank activities cause a severe blur in the reconstruction results. We then applied the prewhitened beamformer in Eq. (13), and the results are shown in Fig. 4(c). Here, $\boldsymbol{R}_{i+n}$ was obtained using the whole prestimulus period. The third source is removed and the blur caused due to the background activity is significantly reduced. We also applied covariance difference beamformer in Eq. (17), and the results are shown in Fig. 4(d). Here, again, the influence of the background activity is significantly reduced. The results in 4(c) (d) clearly demonstrate the effectiveness of the proposed beamformer methods.

References

[**1**] S. E. Robinson, and J. Vrba, "Functional neuroimaging by synthetic aperture magnetometry (SAM)," *Recent Advances in Biomagnetism*, Sendai, pp., 302–305, Tohoku University Press.

[**2**] B. D. van Veen, W. van Drongelen, M. Yuchtman, and A. Suzuki, "Localization of brain electrical activity via linearly constrained minimum variance spatial filtering," *IEEE Trans. Biomed. Eng.*, vol. 44, pp. 867–880, 1997.

[**3**] J. C. de Munck, P. C. M. Vijn, and F. H. Lopes da Silva, "A random dipole model for spontaneous brain activity," *IEEE Trans. Biomed. Eng.*, vol. 39, pp. 791–804, 1992.

[**4**] B. Lütkenhöner, "Magnetic field arising from current dipoles randomly distributed in a homogeneous spherical volume conductor," *J. Appl. Phys.*, vol. 75, pp. 7204–7210, 1994.